

Dual use of rectangular and triangular waveforms in voltammetry using a carbon fiber microelectrode to differentiate norepinephrine from dopamine

Takayuki Jo ¹, Kenji Yoshimi ^{2*}, Toshimitsu Takahashi ³, Genko Oyama¹ and Nobutaka Hattori ¹.

¹ Department of Neurology, Juntendo University School of Medicine, Bunkyo-ku, Tokyo 113-8421, Japan

² Department of Neurophysiology, Juntendo University School of Medicine, Hongo 2-1-1, Bunkyo-ku, Tokyo 113-8421, Japan

³ Dynamic Brain Network Laboratory, Graduate School of Frontier Biosciences, Osaka University, Osaka, 565-0871 Japan.

Abstract: While dopamine (DA) may be clearly detected by voltammetric techniques such as fast-scan cyclic voltammetry (FSCV) in the heavily-innervated striatum, the differentiation of DA from other monoamines, including norepinephrine (NE) and serotonin (5-HT), is crucial for further applications outside of the striatum. We show that using normal pulse voltammetry (NPV) with 0.1 V to 0.3 V rectangular pulses can differentiate between NE and DA. While the major electrochemical current of NE and DA is obtained on 0.2 V rectangular pulse of NPV, the relative current on 0.1 V pulse was higher for DA than NE. It was possible to differentiate NE from DA by electrochemical current on three NPV pulses using simple mathematics of sequential equation. Since FSCV obtains a larger current value and less noisy results than NPV, we alternately recorded both. The electrochemical current data of NPV was combined with FSCV for principal component regression (PCR) analysis. The estimated value was evaluated by percent error and correlation coefficient from the true concentration, and the slope of the linear regression line. Estimation by sequential equation using NPV results could differentiate NE from DA, while PCR without NPV current data could not. PCR including NPV current data also could differentiate NE from DA. In this study, we compared the performance of electrochemical recordings with rectangular and triangular waveforms under the same conditions, and the advantages and disadvantages became very clear. Together with our previous finding of significant differentiation of pH changes from monoamines on rectangular pulses of NPV, the combined use of rectangular and triangular pulses would improve the molecular identification of monoamines in the brain using voltammetric recording.

Key words

Dopamine, norepinephrine, normal pulse voltammetry, FSCV, rectangular pulse

1. Introduction

The usefulness of fast-scan cyclic voltammetry (FSCV) for the detection of dopamine (DA) release in the rat striatum has been established [1,2,3]. It is not only widely used today in rats [4,5], but it is also capable of detecting the reward-associated DA release in behaving mice [6] and monkey striatum [7]. Important cognitive roles of DA in the prefrontal cortex (PFC) have been suggested [8,9], particularly in primates. In addition to the PFC, the rapid DA release in various locations of the brain, such as the hippocampus [10,11], are awaiting a means of detection. For its application in the PFC or the hippocampus, however, DA should be distinguished from other monoamines like norepinephrine (NE) and serotonin (5-HT). In the striatum, the monoamine-like signal has simply been assumed to be DA because of its overwhelming concentration. However, the relative concentration of DA is close to those of NE and 5-HT in the PFC or the hippocampus [12].

The segregation of NE from DA is impossible with FSCV because the voltage-current waveforms of NE and DA are identical [3]. The voltammetric detection of NE on a carbon fiber microelectrode has been performed by FSCV [13,14,15], along with other voltammetric techniques [16,17,18]. Efforts to record NE and DA in the different part of the brain has also been tried [15], but the differential recording of two monoamines at the same recording location has not been possible by standard techniques.

While FSCV applies triangular potential scan, rectangular potentials are also used for voltammetric techniques, including normal-pulse voltammetry (NPV), differential pulse voltammetry and chronoamperometry. We have shown the usefulness of voltammetry using rectangular pulse for fine chemical differentiation [19,20,21,22,23,24]. Rectangular pulse is useful for the segregation of changes in 5-HT from DA [19,20,24]. The voltage dependency of an electrochemical reaction is the basic principle behind chemical identification by voltammetric recordings, and NPV is more effective for finer identifications of voltage dependencies, because the NPV waveform has a period with constant voltage. With fast voltage sweeping in FSCV, the voltage selectivity can be temporally skewed due to electrochemical kinetics, although the peak current amplitude is enhanced. When fine chemical identification is required, NPV would be helpful, and it may assist in differentiating NE and DA. During our previous study (Yoshimi 2014 [20]), we noticed a minor difference in the responses of NE and DA on a 0.1 V rectangular pulse (unpublished observation). In the present study, we sought to use this method for the quantitative estimation of NE and DA. In this study, to take advantage of the high sensitivity of fast-scan cyclic voltammetry (FSCV) and the fine chemical identification of normal pulse voltammetry (NPV), we attempted to combine both techniques on a single carbon fiber. Here, we show the

differentiation of NE from DA using an alternative dual recording of FSCV and NPV.

2. Materials and Methods

2.1. Electrodes.

Carbon-fiber microelectrodes were prepared based on our previous procedures [6,7,19,20,21,22,23,24]. Individual 7 μm diameter carbon fibers (HTA-7, Toho Tenax Co. , Tokyo, Japan) were sealed in pulled glass capillary tubes with an epoxy-resin such that 0.25 mm of the carbon fiber protruded from the capillary tube. The reference and counter (auxiliary) electrodes were Ag/AgCl wires.

2.2. Chemicals.

Chemical reagents including dopamine HCl (DA), norepinephrine (NE), serotonin HCl (5-HT), 3,4-dihydroxyphenylacetic acid (DOPAC), and homovanillic acid (HVA) were purchased from Sigma Aldrich (St. Louis, MO, USA). Ascorbate, uric acid and other special-grade reagents were purchased from Wako Pure Chemicals (Tokyo, Japan). Artificial cerebrospinal fluid (ACSF) for medical use (ARTCEREB, Otsuka, Tokyo, Japan: 145mM Na⁺, 129 mM Cl⁻, 2.8 mM K⁺, 1.1 mM Mg²⁺, 1.15 mM Ca²⁺, 23.1 mM HCO₃, 1.1 mM phosphate, and 0.61 g/L glucose) was purchased commercially and bubbled with 5% CO₂/95% O₂ gas for over 0.5 h until measurement to stabilize the pH, as described previously [20].

2.3. Electrochemistry.

Two types of electrochemical recordings were performed alternately in this study: FSCV and NPV (Figure 1A). The carbon fiber microelectrode was switched between channel 0 and channel 1 of the multi-channel potentiostat (Model HECS-9139, Huso Electrochemical Systems, Kawasaki, Japan). The Ag/AgCl wires for reference and counter electrodes were common for FSCV and NPV recordings. For pulse control and data acquisition, a commercial control/recording system (TH-1; ESA Biosciences, Inc., MA USA) with two multifunction boards (NI-PCI-6221, National Instruments, TX, USA) integrated with a Windows PC was used. The voltage waveform for FSCV was generated by the TH-1, while the three-step rectangular pulses were generated by a pulse generator (MASTER-9, AMPI, Israel). Since the amplitude of the background current was much higher in FSCV, the gain of the amplifier was switched between the FSCV and NPV recordings. The gain of the amplifier was 200 nA/V with a low-pass filter (LPF) of 0.2 ms time constant for FSCV and 20 nA/V with a LPF of 2.0 ms for NPV, as has been described previously [20]. Relatively long time constant of LPF was selected for NPV because the average of 20 ms of time window represent a NPV pulse (Figure 1D) and noise can be lowered with the longer time constant

[20]. The shorter time constant of 0.2ms was selected for FSCV because fine temporal change over 8.5ms of triangular wave is essential for characterization of the chemicals [1,2,3]. The actual current recording was made during an 81-ms time window, as indicated by the magenta and green horizontal bars in Figure 1B. The switching of the potentiostat channels was made at the end of the recordings (red triangles in Figure 1B). For the *in vitro* evaluation of the current responses of the chemicals, carbon fiber microelectrodes were placed in a flow of phosphate-buffered saline (PBS; 0.9% NaCl, 100mM phosphate-buffer pH 7.3), and the flow was switched to test the solutions. Triangular and rectangular voltage pulses were applied alternately on the single carbon-fiber microelectrode (Figure 1B). For FSCV, a triangle waveform lasting 8.5 ms was applied. The potential was ramped from -0.4 V to 1.3 V vs the Ag/AgCl reference and back from 1.3 V to -0.4 V at 400 V/s. For NPV, 25 ms potential steps were given from 0 to 0.1, 0.2 and 0.3 V. Sequentially combined waveforms of 200 ms were applied at 5 Hz.

2.4. Data analysis.

The electrochemical current after the application of the chemicals was analyzed and is represented as background-subtracted currents. To remove the background currents, we subtracted the mean of 10 waveform application baselines just before the application of the test chemicals.

First, the three-step current values of NPV was applied for the estimation of the content, by simple simultaneous equation mathematics. It is based on the characteristic ratio of the averaged current values for each chemical. For the NPV current, an average current of 5 to 25 ms from the voltage pulse onset represented the response at each potential (Figures 1D, 2B). This time window provides the pH-free electrochemical current of monoamines (Yoshimi 2014 [20], also Supplementary Figure S3C). The estimated contents of monoamines were obtained from background-subtracted electrochemical current values at 0.1, 0.2 and 0.3 V for a 1.0 μM standard solution. The ratio of the averaged current of 0.1V to 0.2 V was approximately 0.3 for NE but 0.6 for DA. The estimated concentration of the unknown sample was calculated by pseudo-inverse matrix on MATLAB as [Estimated (μM)] = $\text{pinv}([\text{Std}(\text{nA}/\mu\text{M})]) \times [\text{measured}(\text{nA})]$. For example, the standard current values of three rectangular pulses are given as [0.6 0.8 0.4] nA for DA 1 μM , [0.3 0.8 0.4] nA for NE 1 μM and [0.1 0.1 0.9] nA for 5-HT 1 μM . Then, a measured current set of an unknown sample is given like [0.75 1.2 0.6] nA. The estimation is calculated as DA 1.0 μM NE 0.5 μM and 5-HT 0.0 μM .

The FSCV background-subtracted current was analyzed using principal component regression (PCR) analysis [3]. Principal component procedures were employed using a

custom-made MATLAB program using the “princomp” function. PCR analysis was made either 1: using FSCV only or 2: combining both FSCV and NPV results (dual analysis). For the dual analysis, the three averaged NPV current values were magnified to adjust the original current amplitude difference between FSCV and NPV (Supplementary Figure S1). A magnification constant of 1000 was applied for the presented analysis.

More precisely, a combined vector set of FSCV and NPV was prepared for each time point of every 200ms recording. The procedures were as follows: 1) calculate background current for both FSCV and NPV by averaging the original currents (Figure 1C and D) just before the application of the sample chemicals (5-6 s during a typical 20 s recording); 2) extract voltage-dependent background-subtracted current of 100 points (for 10 ms at 10 kHz) on the triangular waveform of FSCV (Figure 2A); 3) extract background-subtracted current of NPV (Figure 2B); 4) calculate the average of 200 points within each 20 ms time-window (blue bars, Figures 1D and 2B) for the rectangular pulse of NPV; 5) multiply the three averages by the magnification factor (Supplementary Figure S1); and then 6) combine the 100 FSCV points and 3 NPV points to form a vector of 103 points. Averaging the 20 ms time-window was effective for NPV data because the original background-subtracted current of NPV is relatively noisy due to its low amplitude (Yoshimi 2014 [20], also see Supplementary Figure S3). For the template waveforms of PCR, the background-subtracted waveforms of 0.25, 0.5, 1.0 and 2.0 μM of single monoamine solutions (DA, NE and 5-HT, a total of 24 waveform templates after duplicated recordings) were applied. In this study, to maximize the performance of the estimation, the standard template of the analysis was acquired on the same electrode on the same experimental day. In PCR analysis of single monoamine solutions on three carbon fibers, more than 99.6% of variance was captured by three factors. For PCR of FSCV alone, 95.6, 4.0 and 0.2% (average of three electrodes) was captured for the 1st, 2nd and 3rd factors respectively, while they were 69.5, 28.8 and 1.7% for dual PCR with magnification factor of 1000. Since the analysis depends on relatively fine voltage step differences, the actual applied potential of the potentiostat was confirmed carefully for each experiment.

3. RESULTS

3.1. Background current of FSCV and NPV.

The background currents during the measurement are shown in Figure 1C. Since the amplitude of the background current was much higher in FSCV, the gain of the amplifier was switched between the FSCV and NPV recordings. The same background current in Figure 1C is shown in 1D on a different scale. The blue 10 ms horizontal bar in 1C indicates the duration of the analysis of the FSCV current, while the blue bars in 1D indicate three 20 ms windows for the analysis of the NPV current. In this study, the initial large current at the onset of the rectangular pulse was not included in the analysis, because it is pH-sensitive [20].

3.2. Electrochemical current of monoamines.

The background-subtracted current waveforms of FSCV and NPV pulses are shown in Figure 2. The current waveforms for DA and NE (upper half of Figure 2A and B) were almost identical in FSCV (2A), but a slight difference is observed in the 0.1 V NPV pulse (2B). The waveform for 5-HT (lower half of 2A and B) was apparently different from that of DA in NPV (2B) and on the downward slope in FSCV (2A, 7-9 ms after the FSCV onset). The voltage characteristics of NPV and FSCV are almost the same in more physiological solution of ACSF (Supplementary Figure S2) as in PBS (Figure 2). Additional waveforms of electrochemically active chemicals are presented in Supplementary Figure S3.

3.3. Estimation of the content of the chemicals.

The original concentration of the monoamines in the test solutions was estimated by three procedures. First, sequential equation (SQ) using the ratio of the current on three rectangular NPV pulses, second by widely used PCR analysis of FSCV data on triangular waveforms, and third with dual PCR analysis using current data on both rectangular and triangular waveforms.

The estimation by SQ (Figure 3 top) differentiated NE and DA, although a small amount of NE is over-estimated in pure DA sample. An example of PCR estimation by FSCV alone (Figure 3 middle) showed less noisy curve, but DA and NE were not differentiated. Interestingly, the sum of DA and NE (CA) was estimated properly. The result of PCR can be influenced by the variance of the templates. Another example of estimation by FSCV-alone PCR gave proper estimation of DA sample but more than half part of NE sample was taken as DA. When the current of NPV was also included for dual-PCR with magnification factor of 1000 (Figure 3 bottom), NE and DA were differentiated but the curve was noisy, like the estimation by SQ. In all of three estimation procedures, 5-HT was adequately

differentiated. The differentiation of DA and NE were unstable when we tried to estimate DA and NE using FSCV alone.

3.4. Evaluation of the estimation performance.

The results of recording the single and mixed monoamine solutions are summarized in Figure 4 and Table 1. The current value 5 s after the solution change was used for the analysis. Single NE, DA and 5-HT solutions of 0.25, 0.5, 1.0 and 2.0 μ M were tested (Figure 4A, C and D). Also, 1.0 μ M of DA solutions including 0.5, 1.0 and 2.0 μ M NE were also evaluated (4B).

An example using one carbon fiber (Figure 4), the solutions of single NE lead to an estimation that is approximately half the amount of both NE and DA using FSCV alone (A and C). The SQ and dual PCR analysis of the same recording estimated NE without contamination from the DA or 5-HT signals (A). When the NE concentration was increased in the 1.0 μ M DA (B), most of the additional NE was counted as an increase of the DA concentration by FSCV alone (B top). The total CA, the sum of DA and NE values by FSCV alone, was a reasonable estimation. By SQ and dual PCR, both the increasing NE concentrations and the 1.0 μ M DA were reasonably estimated (4B, bottom). Single DA and single 5-HT were reasonably estimated by both methods (4C and D).

The dose dependency between the true concentration of the solution and the estimated results was statistically evaluated by %error, correlation coefficient, and the slope of the regression line (Table 1). The results from three electrodes (Table 1) showed a fine estimation of total CA and 5-HT for the FSCV alone results, small %error, high correlation coefficient and slope close to 1.0. For the SQ and dual-PCR results, DA, NE and 5-HT were estimated properly.

4. DISCUSSION

The differential detection of NE and DA was performed using 0.1, 0.2 and 0.3 V NPV alternating with FSCV. The characteristic of the voltage responses seems to be identical in a more physiological condition of ACSF as in PBS. NPV was useful for the differentiation of NE and DA, but the result was noisier than FSCV. It is important to note that FSCV can estimate total CA and its sensitivity is high. Two-step approach, detect total CA with FSCV first, and second estimate the ratio of NE and DA with NPV information, may be another practical application. This alternating technique of NPV and FSCV should be useful for the differential detection of monoamines outside the striatum.

Further improvement in the mathematical estimation for chemical identification and the sensitivity remains. In this study, we analyzed only the 5 to 25 ms time window of NPV for the calculation, which is insensitive to pH changes [20] (also Supplementary Figure S3C). For a more specific detection in this time window, the amplifier gain can be increased for a higher sensitivity (for example, the present 20 nA/V can be changed to 2 nA/V). Alternatively, when a pH change can be neglected, a higher monoamine current at the onset of each rectangular step (Fig 2C) can be included in the analysis. In addition to NPV supplementing the chemical selectivity of FSCV, it is likely that the large triangular pulses from FSCV enhance the performance of NPV since high-amplitude pulses improve the endurance of carbon fiber sensitivity in NPV [21].

The question of whether the technique introduced in this study is practically useful for multi-monoamine detection in the prefrontal cortex or the hippocampus will be addressed in a future study. There is only a slight difference between NE and DA with a 0.1 V pulse, while the waveform of 5-HT is apparently different from that of DA (Figure 2B). There is no doubt that the differentiation of NE and DA is more challenging than the differentiation of 5-HT and DA. To confirm the performance of NPV in the brain *in vivo*, selective manipulation of midbrain DA neurons or the NE neurons in locus coeruleus using an optogenetic technique [22,25] would be most effective. Combinational use of pharmacological [14,15,16] and electrochemical differentiation technique would synergistically improve the chemical identification.

5. CONCLUSIONS

In summary, it has become possible to distinguish NE and DA by voltammetric recording using a single carbon fiber, and it would be useful to expand the application of this technique to areas outside the striatum. Apart from NE, the addition of the fine voltage selectivity of NPV to FSCV could be widely applicable for improving the chemical

identification of other molecules.

Acknowledgement

The authors thank Adam Weitemier of RIKEN BSI and Shintaro Nagano of Tokyo Metropolitan Institute of Medical Science, for valuable discussions, and Takato Akiba for experimental supports. This study was supported by Juntendo University Research Institute for Diseases of Old Age (a MEXT-Supported Program for the Strategic Research Foundation at Private Universities), and Juntendo University Young investigator joint project award 2015 (2701). We have no financial relationships to disclose.

Supplementary Information

[Supplementary Figure S1. Effect of magnitude ratio for dual-PCR analysis.](#)

[Supplementary Figure S2. Electrochemical current of monoamines in ACSF.](#)

[Supplementary Figure S3. Background-subtracted current waveforms of electrically active chemicals.](#)

Figure Legend

Figure 1. Alternating dual voltammetry method.

(A) Switching circuit for the alternating dual voltammetric recording. The two channels of a multi-channel potentiostat with different settings were switched alternately. A triangular FSCV waveform was directly applied from TH-1 DAQ, while rectangular pulses for NPV were generated by the MASTER-9 triggered by the DAQ. (B) Combined waveform for the alternating dual recording of FSCV and NPV. The timings of the relay switch are indicated with red triangles. The thick horizontal bars indicate the recording duration of FSCV by Ch0 (magenta) and NPV by Ch1 (green). The FSCV part was recorded with a 200 nA/V amplifier with a 0.2 ms LPF, while 20 nA/V with 2.0 ms LPF was applied for the NPV part. The combined waveform was applied at 5Hz. (C and D) The background currents of the carbon fiber in the PBS. The thick light-blue horizontal bar indicates the duration of current analysis for FSCV (C) and NPV (D). The small electrochemical current was isolated after a background subtraction for both FSCV and NPV.

Figure 2. Electrochemical current of monoamines.

A: Current-time curve of the differential current (nA) of FSCV. Shown are 1 μ M of NE (green), DA (blue diamond) and 5-HT (lower, red). The applied potential is also indicated blue dotted line, with the ordinate on the right). B: Current-time curve of the differential current (nA) of NPV. The 20ms time windows are indicated by light-blue lines.

Figure 3. Concentration estimation of single monoamines and the mixture of NE in DA.

Examples of estimated concentration (μ M) of monoamines. The estimation by SQ (top, A to E), by FSCV alone (middle, F to J) and by dual PCR by both FSCV and NPV (bottom, K to O). The PBS solution flow was switched to mixed solution of A, F and K: 1 μ M NE, B, G and L: 1 μ M NE and 1 μ M DA, C, H and M: 2 μ M NE and 1 μ M DA, D, I and N: 1 μ M DA, E, J and O: 1 μ M 5-HT. The estimated value at 5 s after the solution change was used for the later analysis (Figure 4 and Table 1).

Figure 4. Summary of the concentration estimation on a carbon fiber. The abscissa is the real concentration of the test solution, and the ordinate is the estimated concentration. The estimation by SQ (top, A to D), by FSCV alone (middle, E to H) and by dual PCR by both FSCV and NPV (bottom, I to L). From left to right, A, E and I: Various concentrations of single NE, B, F and J: various concentration of NE in 1.0 μ M of DA, C, G and K: single DA, and D, H and L: single 5-HT. Blue open diamond: DA, Green square: NE, red triangle: 5-HT, and black cross shown in E to H: sum of DA and NE (CA). Linear regression lines are

superimposed for NE (A, B, E, F, I and J), DA (C, G and K) and 5-HT (D, H and L). Each symbol indicates estimated value of a single measurement. Note each measurement made three estimation values of DA, NE and 5-HT. Duplicated measurements are shown for each condition. Estimation value 5s from the test solution onset represents each measurement. Three carbon fiber microelectrodes were subjected for identical experiments giving similar results, and summarized in Table 1.

Supplementary Figure S1. Effect of magnitude ratio for dual-PCR analysis.

In order to combine the FSCV and NPV results for dual PCR, NPV value was needed to be magnified, because the original amplitude of NPV was negligible to FSCV. The correlation coefficient between the real concentration and the estimated concentration is shown in ordinate. The data set used 24 background-subtracted waveforms of monoamine samples of 0.25, 0.5, 1 and 2 μM of DA, NE and 5-HT (see Methods). Magnitude 1000 was applied for dual analysis shown in this article.

Supplementary Figure S2. Electrochemical current of monoamines in ACSF.

Background-subtracted differential current of 2 μM NE and DA during dual recording of FSCV and NPV. The carbon fiber microelectrode was placed in the flow of ACSF and switched to a solution with 2 μM of monoamines after 10 s of recording. Top (A and B): NE, and bottom (C and D): DA. A and C: FSCV results of waveform (left) and the current at the peak oxidation potential. B and D: Responses at three-step rectangular pulses (blue diamond: 0.1 V, magenta square: 0.2 V and yellow triangle: 0.3 V).

Supplementary Figure S3. Background-subtracted current waveforms of electrically active chemicals.

Current curves of A: DOPAC (10 μM) and HVA (10 μM), B: ascorbic acid (AA, 10 μM) and uric acid (UA, 10 μM), and C: acidic (pH 6.9) and basic (pH7.8) pH shift from pH 7.3 PBS. Left: FSCV and right: NPV. A: The waveform of DOPAC and HVA, two of metabolites of DA, showed FSCV waveforms similar to DA but NPV waveforms are characteristic. B: Uric acid was similar to 5-HT, but ascorbate showed oxidation current over broad voltage range. C: The waveforms of pH change was broad in FSCV but restricted in the initial 5 msec of each rectangular pulses, as we have shown before (Yoshimi 2014 [20]).

REFERENCES

- [1] R.M. Wightman, C. Amatore, R.C. Engstrom, P.D. Hale, E.W. Kristensen, W.G. Kuhr, L.J. May, Real-time characterization of dopamine overflow and uptake in the rat striatum, *Neuroscience* 25(2) (1988) 513-23.
- [2] K.T. Kawagoe, J.B. Zimmerman, R.M. Wightman, Principles of voltammetry and microelectrode surface states, *J Neurosci Methods* 48(3) (1993) 225-40.
- [3] M.L. Heien, M.A. Johnson, R.M. Wightman, Resolving neurotransmitters detected by fast-scan cyclic voltammetry, *Anal Chem* 76(19) (2004) 5697-704.
- [4] P.E. Phillips, G.D. Stuber, M.L. Heien, R.M. Wightman, R.M. Carelli, Subsecond dopamine release promotes cocaine seeking, *Nature* 422(6932) (2003) 614-8.
- [5] M.P. Sadoris, F. Cacciapaglia, R.M. Wightman, R.M. Carelli, Differential Dopamine Release Dynamics in the Nucleus Accumbens Core and Shell Reveal Complementary Signals for Error Prediction and Incentive Motivation, *J Neurosci* 35(33) (2015) 11572-82.
- [6] S. Natori, K. Yoshimi, T. Takahashi, M. Kagohashi, G. Oyama, Y. Shimo, N. Hattori, S. Kitazawa, Subsecond reward-related dopamine release in the mouse dorsal striatum, *Neurosci Res* 63(4) (2009) 267-72.
- [7] K. Yoshimi, S. Kumada, A. Weitemier, T. Jo, M. Inoue, Reward-Induced Phasic Dopamine Release in the Monkey Ventral Striatum and Putamen, *PLoS One* 10(6) (2015) e0130443.
- [8] M. Watanabe, T. Kodama, K. Hikosaka, Increase of extracellular dopamine in primate prefrontal cortex during a working memory task, *J Neurophysiol* 78(5) (1997) 2795-8.
- [9] T. Sawaguchi, P.S. Goldman-Rakic, The role of D1-dopamine receptor in working memory: local injections of dopamine antagonists into the prefrontal cortex of rhesus monkeys performing an oculomotor delayed-response task, *J Neurophysiol* 71(2) (1994) 515-28.
- [10] J.K. Seamans, C.R. Yang, The principal features and mechanisms of dopamine modulation in the prefrontal cortex, *Prog Neurobiol* 74(1) (2004) 1-58.
- [11] N. Granado, O. Ortiz, L.M. Suarez, E.D. Martin, V. Cena, J.M. Solis, R. Moratalla, D1 but not D5 dopamine receptors are critical for LTP, spatial learning, and LTP-Induced arc and zif268 expression in the hippocampus, *Cereb Cortex* 18(1) (2008) 1-12.
- [12] C. Piffl, G. Schingnitz, O. Hornykiewicz, Effect of 1-methyl-4-phenyl-1,2,3,6-tetrahydropyridine on the regional distribution of brain monoamines in the rhesus monkey, *Neuroscience* 44(3) (1991) 591-605.
- [13] P. Palij, J.A. Stamford, Real-time monitoring of endogenous noradrenaline release in rat brain slices using fast cyclic voltammetry: 1. Characterisation of evoked noradrenaline efflux and uptake from nerve terminals in the bed nucleus of stria terminalis, pars ventralis, *Brain Res* 587(1) (1992) 137-46.

- [14] J. Park, B.M. Kile, R.M. Wightman, In vivo voltammetric monitoring of norepinephrine release in the rat ventral bed nucleus of the stria terminalis and anteroventral thalamic nucleus, *Eur J Neurosci* 30(11) (2009) 2121-33.
- [15] J. Park, P. Takmakov, R.M. Wightman, In vivo comparison of norepinephrine and dopamine release in rat brain by simultaneous measurements with fast-scan cyclic voltammetry, *J Neurochem* 119(5) (2011) 932-44.
- [16] M.F. Suaud-Chagny, C. Mermet, F. Gonon, Electrically evoked noradrenaline release in the rat hypothalamic paraventricular nucleus studied by in vivo electrochemistry: characterization and facilitation by increasing the stimulation frequency, *Neuroscience* 34(2) (1990) 411-22.
- [17] C. Dugast, R. Cespluglio, M.F. Suaud-Chagny, In vivo monitoring of evoked noradrenaline release in the rat anteroventral thalamic nucleus by continuous amperometry, *J Neurochem* 82(3) (2002) 529-37.
- [18] L. Yavich, P. Jakala, H. Tanila, Noradrenaline overflow in mouse dentate gyrus following locus coeruleus and natural stimulation: real-time monitoring by in vivo voltammetry, *J Neurochem* 95(3) (2005) 641-50.
- [19] T. Nakazato, A. Akiyama, High-speed voltammetry: dual measurement of dopamine and serotonin, *J Neurosci Methods* 89(2) (1999) 105-10.
- [20] K. Yoshimi, A. Weitemier, Temporal differentiation of pH-dependent capacitive current from dopamine, *Anal Chem* 86(17) (2014) 8576-84.
- [21] A. Akiyama, T. Kato, K. Ishii, E. Yasuda, In vitro measurement of dopamine concentration with carbon fiber electrode, *Anal Chem* 57(8) (1985) 1518-22.
- [22] T. Danjo, K. Yoshimi, K. Funabiki, S. Yawata, S. Nakanishi, Aversive behavior induced by optogenetic inactivation of ventral tegmental area dopamine neurons is mediated by dopamine D2 receptors in the nucleus accumbens, *Proc Natl Acad Sci U S A* 111(17) (2014) 6455-60.
- [23] G. Oyama, K. Yoshimi, S. Natori, Y. Chikaoka, Y.R. Ren, M. Funayama, Y. Shimo, R. Takahashi, T. Nakazato, S. Kitazawa, N. Hattori, Impaired in vivo dopamine release in parkin knockout mice, *Brain Res* 1352 (2010) 214-22.
- [24] A. Suzuki, T.A. Ivandini, K. Yoshimi, A. Fujishima, G. Oyama, T. Nakazato, N. Hattori, S. Kitazawa, Y. Einaga, Fabrication, characterization, and application of boron-doped diamond microelectrodes for in vivo dopamine detection, *Anal Chem* 79(22) (2007) 8608-15.
- [25] K. Janitzky, M.T. Lippert, A. Engelhorn, J. Tegtmeier, J. Goldschmidt, H.J. Heinze, F.W. Ohl, Optogenetic silencing of locus coeruleus activity in mice impairs cognitive flexibility in an attentional set-shifting task, *Front Behav Neurosci* 9 (2015) 286.

Table 1. Statistical summary of estimated concentration.

		NE		DA		CA		5-HT	
%Error	NPV SQ	26.9	±3.4	23.7	±8.7	13.1	±3.2	16.9	±5.0
	FSCV-PCR	130.7	±18.0	112.5	±13.9	22.2	±1.3	13.6	±3.7
	Dual-PCR	35.5	±8.5	21.8	±9.1	16.6	±1.3	16.6	±4.4
Correlation coefficient	NPV SQ	0.982	±0.007	0.990	±0.010	0.988	±0.008	0.996	±0.001
	FSCV-PCR	0.630	±0.078	0.780	±0.161	0.972	±0.003	0.996	±0.001
	Dual-PCR	0.993	±0.007	0.990	±0.011	0.992	±0.007	0.996	±0.002
Slope	NPV SQ	0.92	±0.07	0.88	±0.11	0.84	±0.05	0.85	±0.05
	FSCV-PCR	0.42	±0.09	0.76	±0.35	0.88	±0.07	0.95	±0.00
	Dual-PCR	0.95	±0.02	0.90	±0.10	0.89	±0.06	0.91	±0.03

The %error, the correlation coefficient and the slope of linear regression line of the real and the estimated concentrations at 5s were calculated. The values were calculated from the experiments shown in Figure 4 for each carbon fiber microelectrode. The average and \pm SD of three electrodes are shown. With ideal estimation, the %error would be 0,0, and the correlation coefficient and slope would be 1.0. The %error and correlation coefficient was calculated from the duplicated measurements of 12 kinds of pure monoamine solutions for each carbon fiber microelectrode. CA value is the sum of NE and DA. The slope was calculated from only the value of subjected chemicals (4 concentrations of one kind of chemical, but 8 kinds of NE and DA results were subjected for CA).

Figure1

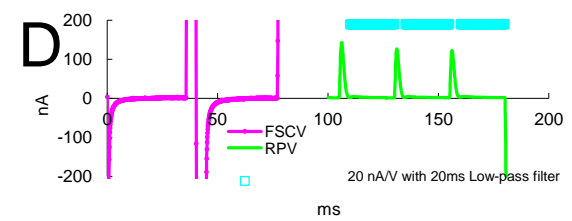
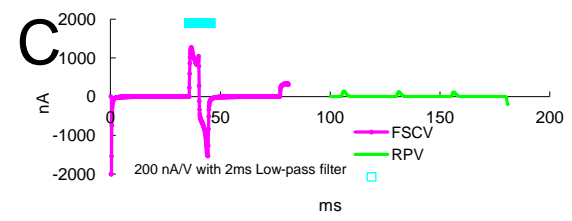
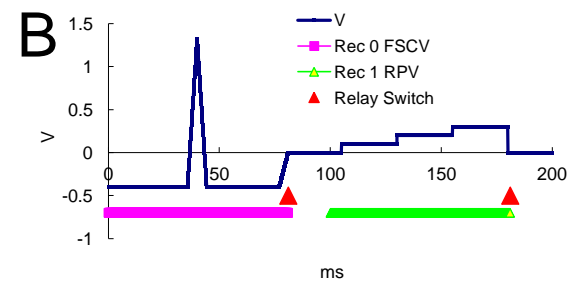
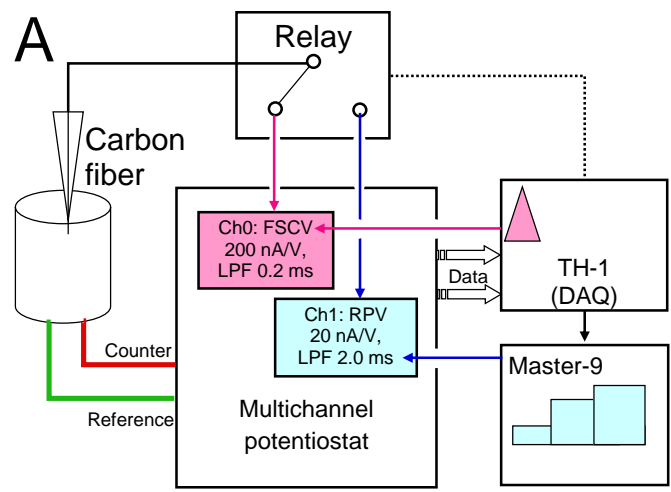


Figure 1

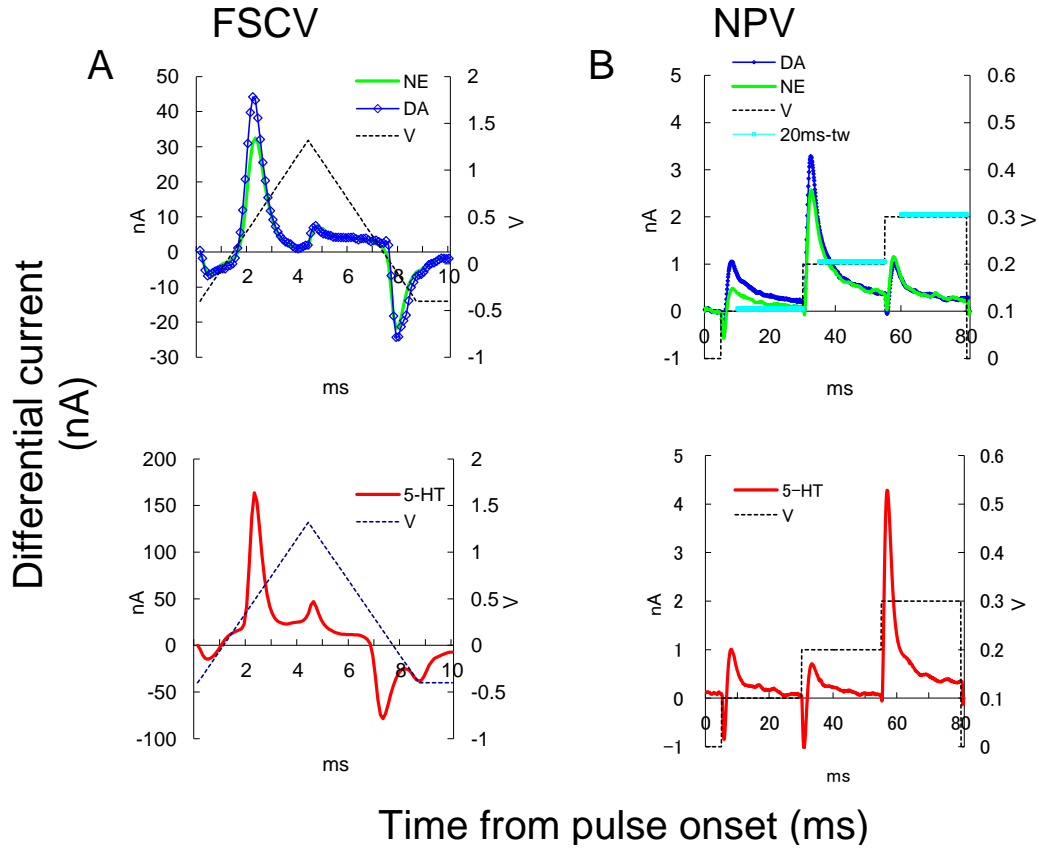


Figure 2

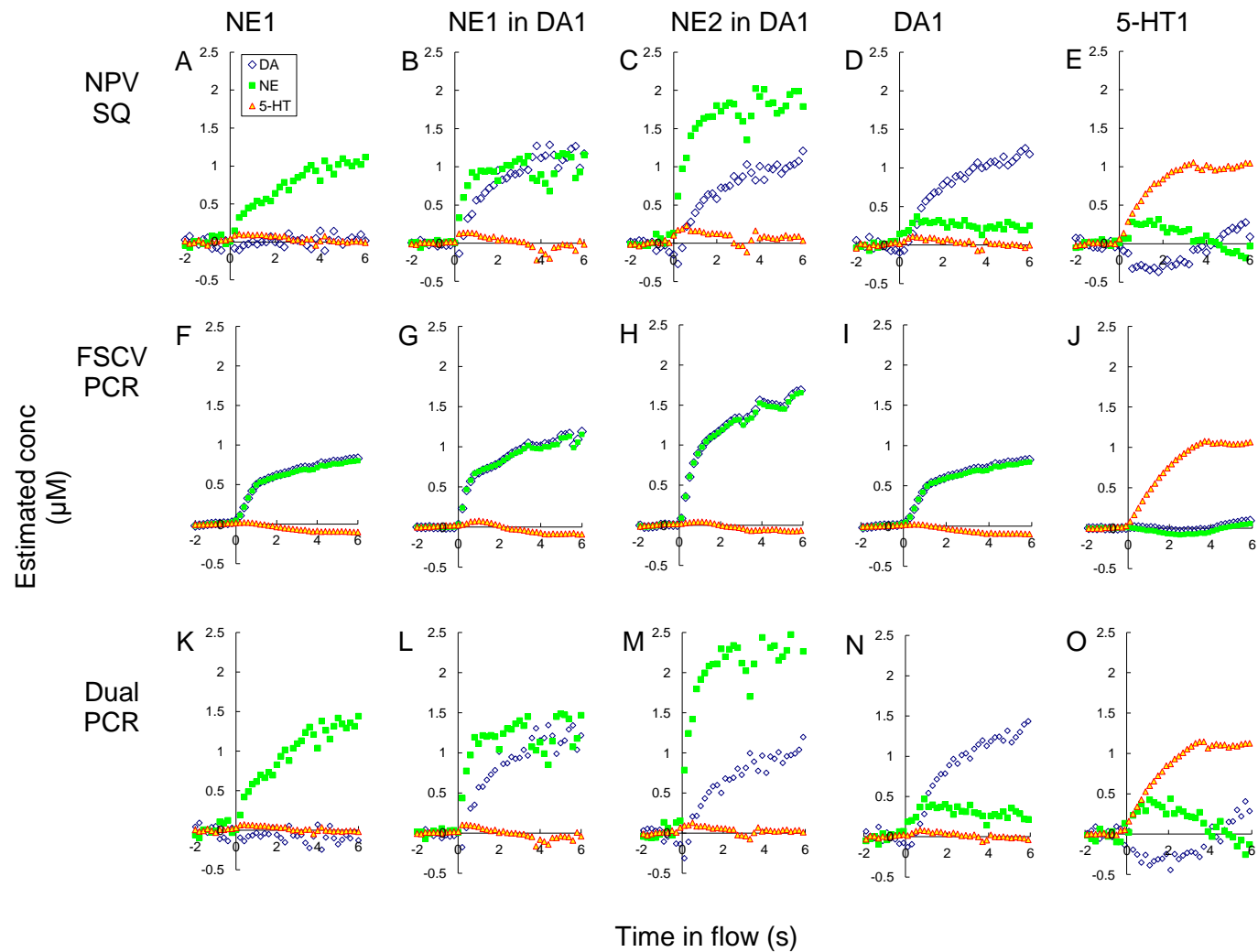


Figure 3

Figure4

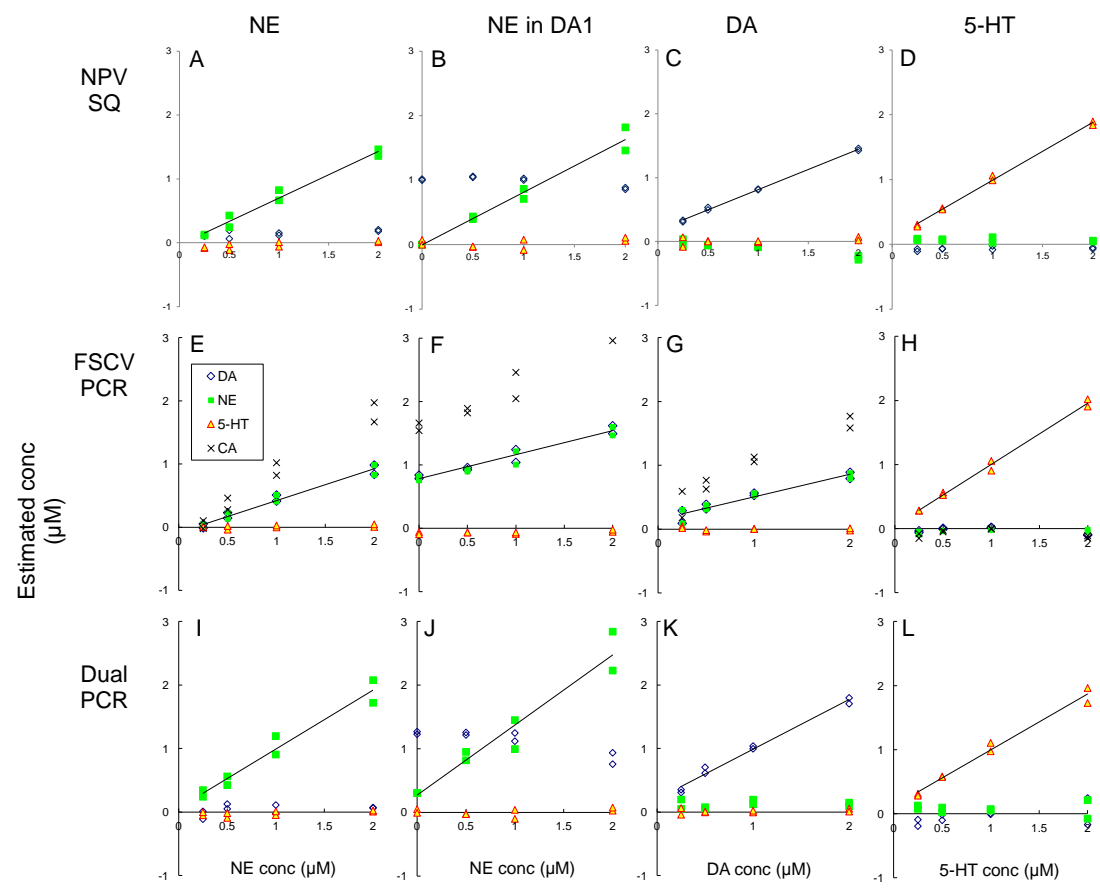


Figure 4

Supplementary Material1

[Click here to download Supplemental material for on-line publication only: SF1.xlsx](#)

Supplementary Material2

[Click here to download Supplemental material for on-line publication only: SF2.xls](#)

Supplementary Material3

[Click here to download Supplemental material for on-line publication only: SF3.xlsx](#)